

A Tendon-Driven Dexterous Hand Design with Tactile Sensor Array for Grasping and Manipulation *

Bin Fang*, Fuchun Sun, Yang Chen and Chang Zhu
*Department of Computer Science and Technology
Tsinghua University
Beijing, China*

{fangbin, fcsun, chenyang, zhuchang}@mail.tsinghua.edu.cn

Ziwei Xia and Yiyong Yang*
*School of Engineering and Technology
China University of Geoscience
Beijing, China*
{3002190019, yangyy}@cugb.edu.cn

Abstract—This paper presents a tendon-driven dexterous hand with tactile sensor array. The proposed modularized dexterous hand that has optimized finger structure, tendon transmission and sensory system is introduced. The tendon path is optimized to reduce friction and the whole composition of finger is more compact. In order to maintain the tension of tendon, a novel tensioner is designed and mounted between the actuators and the hand. Then the high-density tactile sensor array is elaborated. It has the advantages of high measuring accuracy, high-density array, easy to install. Meanwhile, the control system of the dexterous hand is introduced. Finally several experiments are implemented to prove the effectiveness of the proposed tendon-driven dexterous hand.

Index Terms—Tendon-driven. Dexterous hand. Tensioner. Tactile sensor.

I. INTRODUCTION

For decades, robotics hands have been one of the most active areas in robotic literature. Many multi-fingered robotics hands have been designed in labs and companies for various manipulation tasks. Generally they can be separated into three categories: tendon driven hand (DLR/HIT hand[1], PISA/IIT soft hand[2], HERI hand[3]), linkage driven hand (SSSA hand [4], Robotiq hand [5]), worm gearing driven hand (RIC arm-hand [6], RII hand [7]). Currently, most robotics hands utilize tendon driven structure on account of flexibility and simplifying the complexity of robotics hand[8]. Meanwhile, tendon-driven robotics hands' actuators usually fit on the forearm, so the hand and driven mode are independent that would be easier to maintain and repair than other structures. Actually it's obvious that the tendon-driven will attract more attention if it improves performance and reduce cost. Although tendon-driven dexterous hands have made great advances in grasping capacity, response speed, robustness, size etc., the problem about how to trade-offs these requirements is still remained. For instance, DLR Awiwi hand[9] has excellent robustness and grasping performance, but it has complex driven module

and large overall dimension. Shadow hand[10] can accomplish dexterous in-hand manipulation, such as rotate a magic cube or eggs, however the price of Shadow hand is expensive. Thus, we try to design a dexterous hand which making trade-offs between these requirements.

So far, robotics hand's grasping capability mainly depends on mechanical structure and sensory system. Mechanical structure determines flexibility of dexterous hands. Generally, besides thumb, each finger of human has three joints: the metacarpophalangeal (MCP), proximal interphalangeal (PIP), and distal interphalangeal (DIP) joints. It means each finger has 3 DoFs (PIP and DIP have one flexion-extension DoF. MCP has flexion-extension DoF and abduction-adduction DoF) and thumb is even more. Thus anthropomorphic dexterous hands always have at least three DoFs, such as ROBIOSS hand[11], KITECH hand[12]. And the proposed hand in the paper uses the flexion-extension motion to develop the optimal way to achieve accurate finger controlling.

Sensory system is as significant as mechanical structure. It provides the information as tactile, joint angle, force for robotic manipulation. When dexterous hand performs a task, sensors need real-time feedback position information and the situation of contact with objects. Though analysis these information, some complicated task can be performed, such as object position detection[13], slippage detection[14], texture recognition [15] and so on. So optimizing sensors and structure is equally important for design a dexterous hand.

In this paper, the modularized dexterous hand which has been optimized finger structure, tendon transmission and sensory system is presented. For fingers, the structure design is described. Not only tendon path is designed to reduce friction, but also the whole composition of finger is more compact that tactile sensor, joint sensor and data collecting board are assembled in the finger. And in order to maintain the tension of tendon, a novel tensioner is mounted between actuator and hand. To improve the sensor precision, a novel 5*5 arrays tactile sensor is presented which has the advantages of high measuring accuracy, high-density array, easy to install. The organization of the paper is as follows. In Section II, details the structure of our dexterous hand, include

*This work is supported by National Key Research Program of China with Project No. 2018YFB1305603

* are the corresponding authors.

finger module, tendon transmission, kinetic analysis. Section III describes the sensory system of dexterous hand and present a novel design of 5*5 arrays tactile sensor. Section IV introduces the control system. Section V perform many grasping experiments verify the performance of hand. In the Section VI, the conclusion and future work are summarized.

II. STRUCTURE DESIGN AND KINETIC ANALYSIS

Dexterous hand always has many DoFs which for executing complex tasks. Therefore it is necessary to analyze the distribution of degrees of freedom, structure design, grasping and operating state of the dexterous hand. And the performance of dexterous hand greatly depends on its structure.

According to the structure, the fingers of the dexterous hand can be divided into two types: thumb and the remaining four fingers. Thus in this part, both the two types of finger structural design of dexterous hand is introduced respectively. Then based on its structure, the kinematics and motion space analysis of the dexterous hand were carried out.

A. Index finger design

Based on the human hand size and structure, the requirements of fingers should have compact structure and high flexibility. As for index finger, this dexterous hand has the same structure as human hand, it has three parts: proximal, middle and distal segments. The benefit of this modular design is easy to replace and assemble. The overall hand use 1:1.2 scale designed and the total finger length is 110mm. The size of each part is as shown in figure 1. This dexterous hand is driven by tendon, there are two pairs of tendons in index finger. PIP and MIP is driven by one pair of tendons, and MCP is driven by another pair of tendons. The PIP and DIP are coupled motion driven by an actuator, rotated around axis a and axis b respectively. There are two pairs of tendons inside the finger used to control the finger motion (flexion and extension). And each joint's motion space is 0° - 90° . The finger structure is manufactured by 3D print technology, it saves space with compact design that has high anthropomorphism.

Considering the effect of friction between tendon and path, there are three methods use for solve this problem. Each joint is equipped with bearings to reduce the friction when rotation. Each tendon is in teflon tube. On the outside of the pipe, flexible metal tube is covered to protect teflon tube. When tendon though the path which has a large angle, pulley will equip on the path used to decrease friction. With these methods, the friction between tendon and path is reduced.

B. Index finger tendon transmission

The index finger has two pairs of tendon, tendon A (active tendon) and tendon B (passive tendon) fixed on the distal

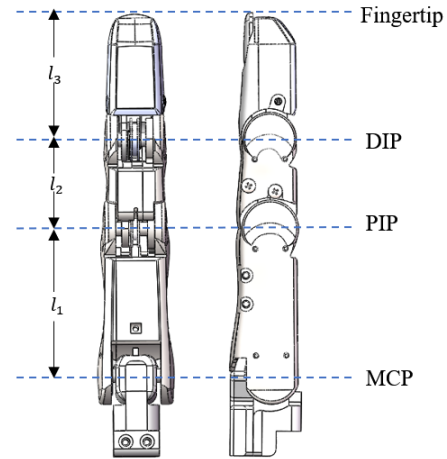


Fig. 1. The prototype of index finger.

segment. Tendon A controls the inflection of distal segment and middle segment. And tendon B is used to control the extension motion. Tendon B connect to actuator which go through DIP, PIP, MCP. And the installation of tendon A is similar with tendon B. The second pair of tendons is fastened to the proximal segment used to control MCP flexion or extension. Because PIP and DIP need to go though MCP joint to control tendons, tendon A and tendon B will affect tendon C and tendon D when they motion. Thus the decoupling of these two DoFs should be carefully considered. Aim at tendon-driven mode, the transmission is optimized. Each tendon is covered with Teflon pipe to reduce friction, and outside the Teflon pipe encase flexible metal tube to protective Teflon pipe not bend inside dexterous hand.

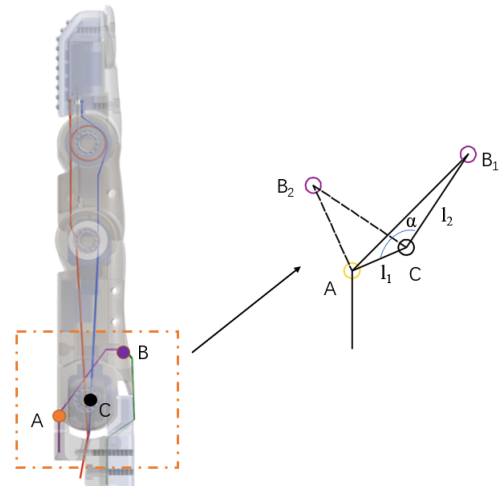


Fig. 2. Index finger tendon transmission.

As shown in figure 2, the MCP structure is simplified. Point A is the point of contact with the finger when the

tendon comes out of the path, point B_1 is the point which MCP tendon is fixed when finger is vertical and point B_2 is the point which MCP tendon is fixed when finger is rotate 90° , point C is the MCP's axis. When finger from initial position to final position, the length between l_{AB_1} and l_{AB_2} is the variation length of the tendon. And using the relation between angle and side on the triangle, the relation between l_{AB} and α can be infer as :

$$l_{AB} = \sqrt{l_{AC}^2 + l_{CB}^2 - 2 * l_{AC} * l_{CB} * \cos(\alpha - \theta)} \quad (1)$$

In this function, α is the initial angle between l_{AC} and l_{CB} , θ change among $0 - 90^\circ$. Based on this equation, the relationship between joint angle and motor motion distance is as shown as figure 3. When actuator motion among 0-9mm, the joint will change among $0-90^\circ$. And the curve is smoothing, it ensures the finger will motion with good continuity.

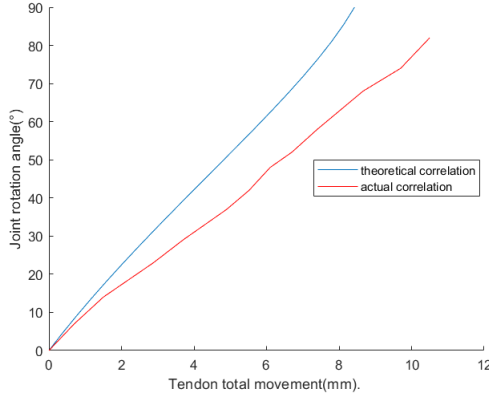


Fig. 3. Relationship between motor and joint

C. Thumb design

Thumb plays an important role in a dexterous hand. And thumb is the most flexible finger which has more DoFs than other finger. When dexterous hand need to perform various tasks, the thumb always cooperate with other fingers. When grasp objects, thumb is usually in a position that relative to other fingers to ensure the stability of the operation.

The thumb structure is as shown in figure 4. It has three joints: PIP, DIP, CMC. Each joint is driven by a actuator independently and can move alone without affecting other joints. Thumb though foundation fixes on palm. All of these three joints can rotate 90° ensure thumb's dexterity.

D. Thumb tendon transmission

Because thumb is more flexible than other four fingers, most hand action need thumb to cooperate with other fingers. Therefore thumb tendon transmission is more complex than

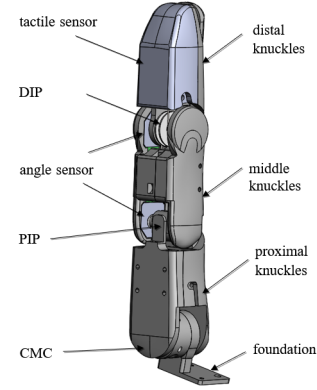


Fig. 4. The structure of thumb

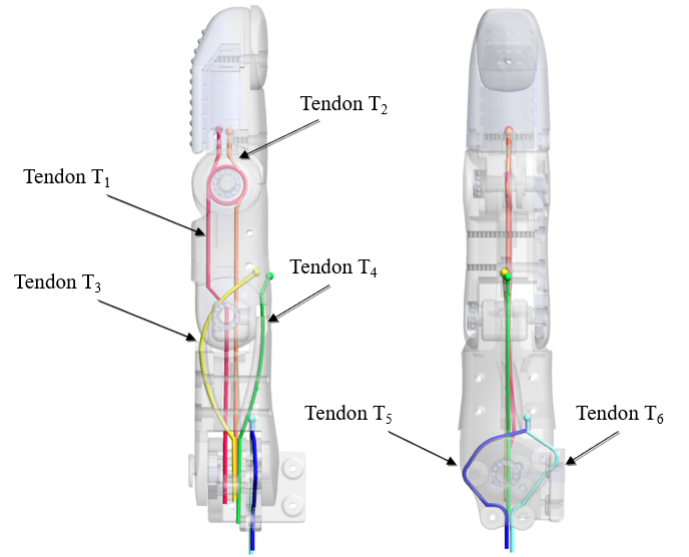


Fig. 5. Thumb tendon transmission.

other fingers. Aim at thumb flexibility, the transmission of thumb tendon is optimized as shown as figure 5.

Tendon T_1 and tendon T_2 control thumb PIP motion, tendon T_3 and T_4 control DIP to rotate and reset. Their install ways is similar to index finger. However thumb has three DoFs, tendon T_5 and T_6 need to control CMC motion without affecting PIP and DIP. Therefore tendon T_5 and T_6 go though thumb axis to connect to actuator, this way can minimize the affect of other joints. At the same time, there are four pulley in thumb CMC to reducing friction and limit tendon path. And tendon T_5 and T_6 are separated from other tendon, thus they don't interfere with others. On account of this transmission design scheme, thumb can work well. Meanwhile, tendon T_5 is tend to strain state when thumb bend, it's conducive to control CMC motion.

E. Driven module design

Driven module is consisted of two parts, one is motor and another is tensioner. Tensioner is important for driven module. Tendon transmission structure is easy to be elongated, so driven module which has no tensioner will affect the control of the dexterous hand. We design a new type of tensioner to keep the tendon tight. The structure is as shown in figure 6.

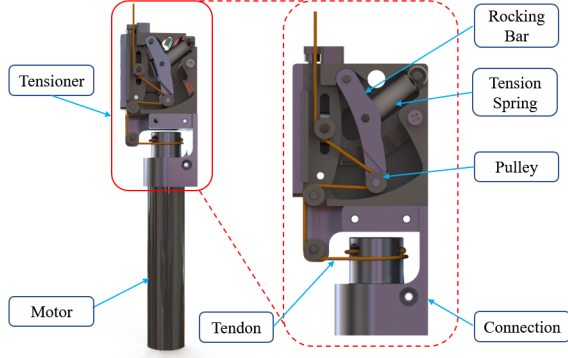


Fig. 6. The prototype of proposed tensioner

Each tendon goes across the inside of the finger. And they are connected to the motor though three pulleys. The connection is used to connect tendon and motor. And the top pulley is adjustable, this design allows the tendons to be fitted firstly and then pre-tightened. The tension spring has certain pretension force, so the tendon always is in state of strain.

Rocking bar can rotate in the tensioner, and the rotation range is about 40° . The rocking bar's length is 25mm, so the tensioner allows tendon has 17.25mm elongation. And when the rope tension reaches a certain value, the tension spring will extension and rocking bar will slick on the left side. After this, the length of tendon changes linearly with the rotation of the motor. And the force which make the rocking bar to the maximum position can be acquired by the tension spring's performance parameter.

Based on this design of the tensioner, the dexterous hand's performance is optimized. And the problem about tendon loose is solved.

F. Motion space of dexterous hand

The proposed dexterous finger can reach a large motion space which similar to the human finger. Each finger's motion space is obtained via D-H parameter method. And each finger's D-H parameters is as shown in table. When grasping, the middle three fingers can be thought of as consisting of multiple revolute joints motion together. Through the motion of each joint, the fingertips reach all positions in the workspace. Thumb workspace intersect with the other four fingers. This result is beneficial for grasping and in-

hand manipulation. The motion space of dexterous hand is as shown in figure 7.

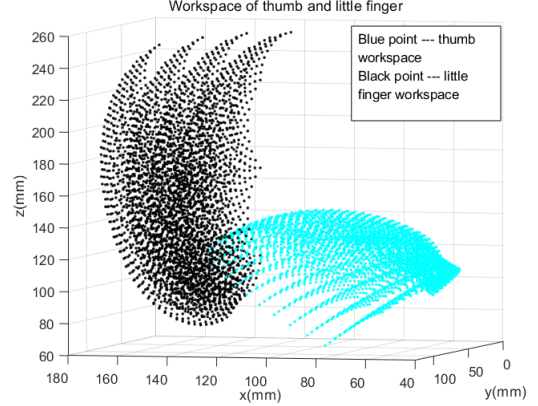


Fig. 7. Workspace of thumb and little finger

TABLE I
D-H PARAMETER OF INDEX FINGER

| Phalange | Length l_i (mm) | Rotation θ_i ($^\circ$) | d_i (mm) | α_i ($^\circ$) |
|------------------|-------------------|----------------------------------|------------|-------------------------|
| Base | 0 | [0,90] | 0 | 0 |
| Proximal segment | 41 | [0,90] | 0 | 0 |
| Middle segment | 26 | [0,90] | 0 | 0 |
| Distal segment | 34 | 0 | 0 | 0 |

TABLE II
D-H PARAMETER OF THUMB

| Phalange | Length l_i (mm) | Rotation θ_i ($^\circ$) | d_i (mm) | α_i ($^\circ$) |
|------------------|-------------------|----------------------------------|------------|-------------------------|
| Base | 0 | [0,90] | 0 | [0,90] |
| Proximal segment | 37 | [0,90] | 0 | 0 |
| Middle segment | 32 | [0,90] | 0 | 0 |
| Distal segment | 42 | 0 | 0 | 0 |

TABLE III
D-H PARAMETER OF LITTLE FINGER

| Phalange | Length l_i (mm) | Rotation θ_i ($^\circ$) | d_i (mm) | α_i ($^\circ$) |
|---------------------|-------------------|----------------------------------|------------|-------------------------|
| Base | 0 | [0,15] | 0 | 0 |
| Metacarpophalangeal | 70 | [0,90] | 17 | [0,40] |
| Proximal segment | 41 | [0,90] | 0 | 0 |
| Middle segment | 26 | [0,90] | 0 | 0 |
| Distal segment | 34 | 0 | 0 | 0 |

III. SENSOR SYSTEM

Each finger joint is equipped with angle sensors, the flexion angle information of each joint can be measured in real time when dexterous hand is working, and the angle information can be collected by the control board. And the fingertip is attached an array of tactile sensor. Thus dexterous hand can receive tactile feedback information, ensure the stability and accuracy of grasping.

A. Tactile sensor

Each of the fingertip is equipped with tactile sensor array, the sensor structure is shown as figure 8. The structure of tactile sensor is consisted of five parts: insulating layer A row electrode, insulating layer, pressure sensitive, insulating layer B, insulating layer B longitudinal electrode. The electrode is contact with pressure sensitive. When ambient pressure of pressure sensitive is changed, value of resistance between layer A and layer B changed with it. In this way of measuring value of resistance, the pressure of sensor is obtained. And layer A electrode is row ,layer B electrode is longitudinal. Therefore pressure sensitive is divided to $n \times n$ matrix form.

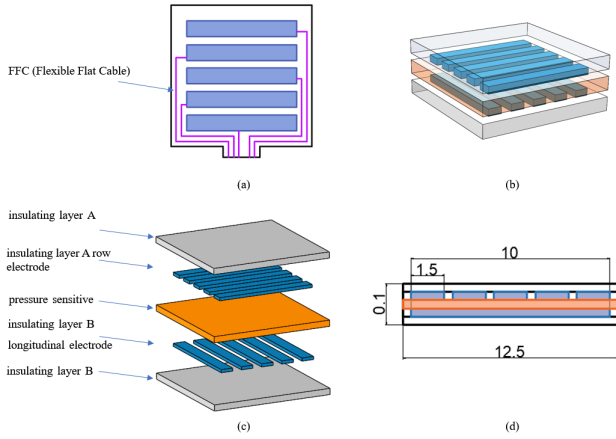


Fig. 8. The prototype of proposed tactile sensor

The equivalent circuit of the pressure sensor is shown as figure 9. Value of resistance of layer A and layer B is related to pressure. Through measure value of resistance, the value of pressure is acquired. Take 2×2 tactile sensor for example, measuring circuit schematic diagram is as shown in figure 9. Electrode A and B is cascading with resistance. Electrode C and D is cascading with resistance, then connect ground. Apply a positive voltage (V_{cc}) to the electrode A and detect A, B, C, D voltage. After that switching voltage between electrode A and B, detect each point voltage again.

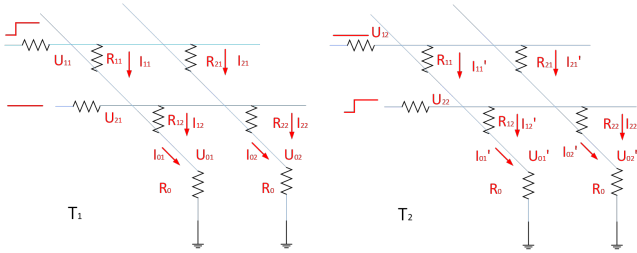


Fig. 9. Two occasions of resistance network state

Set up the equation for the collected voltage value. At T_1 ,

for the circuit on the left side, the following equation can be established:

$$\begin{cases} I_{11} + I_{12} = I_{01} \\ U_{11} - I_{01}R_0 = I_{11}R_{11} \\ U_{21} - I_{01}R_0 = I_{12}R_{12} \end{cases} \quad (2)$$

I_{11} is the current through R_{11} , U_{11} is voltage of point A, U_{21} is voltage of point B, U_{01} is voltage of point C, U_{02} is voltage of point D.

At T_2 , the equation is shown:

$$\begin{cases} I'_{11} + I'_{12} = I'_{01} \\ U_{12} - I'_{01}R_0 = I'_{11}R_{11} \\ U_{22} - I'_{01}R_0 = I'_{12}R_{12} \end{cases} \quad (3)$$

Simultaneous equation can be obtained from Eq.(1) and Eq.(2)

$$\begin{aligned} \begin{cases} U_{11}R_{12} = I_{01}R_0R_{12} + I_{11}R_{11}R_{12} \\ U_{21}R_{11} = I_{01}R_0R_{11} + I_{12}R_{11}R_{12} \end{cases} \\ \Rightarrow U_{11}R_{12} + U_{21}R_{11} = \\ I_{01}R_0R_{12} + I_{11}R_{11}R_{12} + I_{01}R_0R_{11} + I_{12}R_{11}R_{12} \\ \Rightarrow U_{11}R_{12} - I_{01}R_0R_{12} + U_{21}R_{11} - I_{01}R_0R_{11} = \\ I_{11}R_{11}R_{12} + I_{12}R_{11}R_{12} \end{aligned}$$

$$\Rightarrow \frac{U_{11} - I_{01}R_0}{R_{11}} + \frac{U_{21} - I_{01}R_0}{R_{12}} = I_{11} + I_{12} = I_{01} \quad (4)$$

$$\begin{aligned} \begin{cases} U_{12}R_{12} = I'_{01}R_0R_{12} + I'_{11}R_{11}R_{12} \\ U_{22}R_{11} = I'_{01}R_0R_{11} + I'_{12}R_{11}R_{12} \end{cases} \\ \Rightarrow \frac{U_{12} - I'_{01}R_0}{R_{11}} + \frac{U_{22} - I'_{01}R_0}{R_{12}} = I'_{11} + I'_{12} = I'_{01} \quad (5) \end{aligned}$$

Simultaneous Eq.(4) and Eq.(5). Replace variable $I_{01}R_0$ with variable U_{01} as the voltage value at T_1 , and replace variable $I'_{01}R_0$ with variable U_{02} as the voltage value at T_2 . The equation can be expressed as Eq.(6).

$$\begin{aligned} \begin{cases} \frac{U_{11} - I_{01}R_0}{R_{11}} + \frac{U_{21} - I_{01}R_0}{R_{12}} = I_{01} \\ \frac{U_{12} - I'_{01}R_0}{R_{11}} + \frac{U_{22} - I'_{01}R_0}{R_{12}} = I'_{01} \end{cases} \\ \Rightarrow \begin{bmatrix} U_{11} - I_{01}R_0 & U_{21} - I_{01}R_0 \\ U_{12} - I'_{01}R_0 & U_{22} - I'_{01}R_0 \end{bmatrix} \begin{bmatrix} \frac{1}{R_{11}} \\ \frac{1}{R_{12}} \end{bmatrix} = \begin{bmatrix} I_{01} \\ I'_{01} \end{bmatrix} \\ \Rightarrow \begin{bmatrix} U_{11} - U_{01} & U_{21} - U_{01} \\ U_{12} - U_{02} & U_{22} - U_{02} \end{bmatrix} \begin{bmatrix} \frac{1}{R_{11}} \\ \frac{1}{R_{12}} \end{bmatrix} = \begin{bmatrix} I_{01} \\ I_{02} \end{bmatrix} \quad (6) \end{aligned}$$

$$\begin{bmatrix} U_{11} - U_{01} & U_{21} - U_{01} & U_{31} - U_{01} & U_{41} - U_{01} & U_{51} - U_{01} \\ U_{12} - U_{02} & U_{22} - U_{02} & U_{32} - U_{02} & U_{42} - U_{02} & U_{52} - U_{02} \\ U_{13} - U_{03} & U_{23} - U_{03} & U_{33} - U_{03} & U_{43} - U_{03} & U_{53} - U_{03} \\ U_{14} - U_{04} & U_{24} - U_{04} & U_{34} - U_{04} & U_{44} - U_{04} & U_{54} - U_{04} \\ U_{15} - U_{05} & U_{25} - U_{05} & U_{35} - U_{05} & U_{45} - U_{05} & U_{55} - U_{05} \end{bmatrix} \begin{bmatrix} \frac{1}{R_{11}} \\ \frac{1}{R_{12}} \\ \frac{1}{R_{13}} \\ \frac{1}{R_{14}} \\ \frac{1}{R_{15}} \end{bmatrix} = \begin{bmatrix} I_{01} \\ I_{02} \\ I_{03} \\ I_{04} \\ I_{05} \end{bmatrix} \quad (7)$$

TABLE IV
PERFORMANCE OF TACTILE SENSOR

| Performance index | Parameter |
|-------------------|-----------|
| size | 15mm*15mm |
| thickness | 0.2mm |
| resolution ratio | 0.1N |
| range | 0-20N |
| response speed | 1ms |
| rated load | 500N |

Take this method extend to 5*5 array tactile sensor, the result can be shown as Eq.(7), and pressure value can be obtained by $\frac{1}{R_{xy}}$.

Through experiments, the sensor data is obtained when the loading force between 0-20N. The relationship between loading force and sensor data is as shown as figure 10. The sensor data changes smoothly, and though these data the sensor calibration can be accomplished. Base on the result of this experiment, the equation of sensor value curve is obtained.

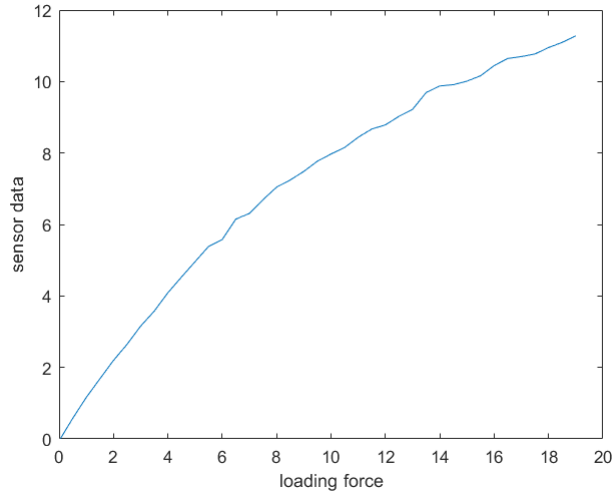


Fig. 10. Characteristic curve of tactile sensor.

B. Angle sensor

Angle sensor is manufactured by Japan, and its type is SV01A103AEA01R00. It is one kind of resistance angle sensor. The sensor is small and fine, with a length of 12mm,

a width of 11mm and a thickness of only 2.1mm. Benefit by its small size, it can be assembled on the joint of the hand without taking up too much space. When installed, the shaft of the dexterous hand joint is enclosed in the inner diameter of the sensor, and the other part is covered by the finger shell. Sensor wire connects from the sensor to the corresponding control board.

IV. CONTROL SYSTEM

A. Motor drive hardware design

The dexterous hand actuated motor structure is used stepping motor and guide screw. Motor step angle is 18° and screw pitch is 0.5 mm, therefore the stepping motor receives a pulse control signal, and the actual stroke of the slider is 0.025mm. The slide block can keep the motor self-locking in case of power failure. The driving structure of a single motor generally includes a driving control board, a light rod, a screw rod, a sliding block steering pulley and a stepping motor. The driving board and control board of the stepping motor are fixed on the lower part of the structure.

The driving part uses a total of 12 driving motors. Motor drive IC is based on TRINAMIC company TMC5130 chip. It has two H bridge circuits and a 1/256 micro step protractor which can drive a bipolar stepping motor. It combines a flexible ramp generator for automatic target positioning with industries' most advanced stepper motor driver. Based on TRINAMICs sophisticated stealthChop chopper, the driver ensures absolutely noiseless operation combined with maximum efficiency and best motor torque. Since there are 12 stepping motors to be controlled, STM32F103R8T6 is selected as the motor control chip, and STM32F103 sends motor control signal input to TMC5130 through SPI interface.

B. Motor control algorithm

The tendon drive mode of the dexterous hand used in this paper is to use the motor to move the finger joint through the tendon rope. However, this kind of transmission has certain defects. When the rope is deformed due to the tension or the friction between the rope and the casing, the system has strong non-linearity, and the accurate joint position control becomes very difficult. The control method of the dexterous hand used in this paper takes tactile array sensor and Angle position sensor as feedback signal input, and uses PID algorithm to realize motor driven finger joint motion control. The control board diagram is shown in figure 11.

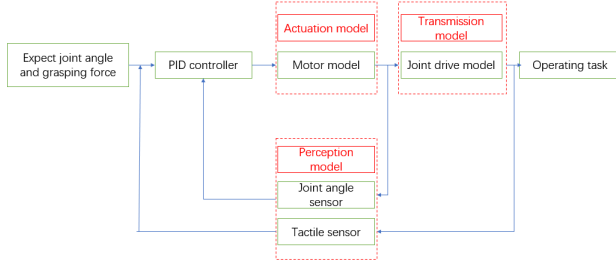


Fig. 11. Drive board PCB diagram

V. EXPERIMENTS

After the design of the structure part, the sensing part and the control system of the dexterous hand is completed, the debugging of the whole control platform should be carried out in combination with the dexterous hand. The dexterous hand performance is verified by a variety of grasp or manipulate experiments which perform by the hand. The proposed five-fingered dexterous robotics hand is shown in Figure 12.



Fig. 12. Open posture of the dexterous hand.

A. Construction of experimental platform

Experimental platform is composed of dexterous hand, the PC(Personal Computer), AC(alternating current) power supply, objects of different shapes(sphere, card, cylinder). Dexterous hand was placed on the desktop before experiment began. And it communicates with PC through USB interface. The upper computer uses dexterous operating interface to send finger movement instructions. The details of experimental platform is as shown in figure. 13

B. Grasping experiments

Though figure 14 and 15 the dexterous hand can accomplish different kinds of power manipulate and precision manipulate. And the hand can grasp various shape objects

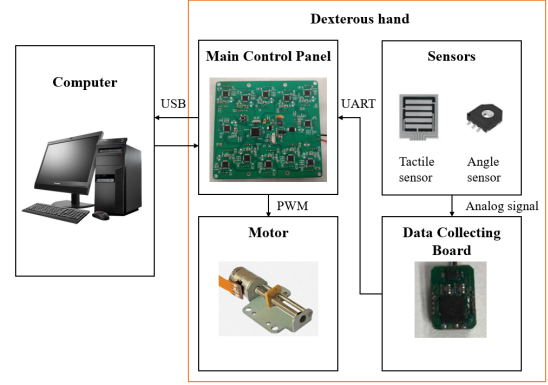


Fig. 13. The details of experimental platform. The main control panel can receive instructions from the computer and uploads the current data of the sensor through USB-UART. The data acquisition board collects the angle value and tactile pressure value through analog signals, quantifies them and transmits them to the main control panel through UART. The main control panel has the function of driving motor. And it can drive 12 motors.

include sphere, cylinder, card. And the maximum diameter of the sphere is 75mm, the minimum diameter of the sphere is 40mm. For cylinder, the bottle's diameter is 80mm and the mango's diameter is 52mm.

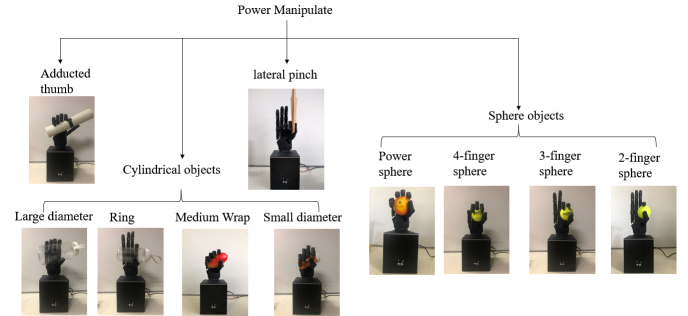


Fig. 14. The experiments of power manipulate.

The dexterous hand designed in this paper is quite flexible and has a large work space to grasp and operate. For objects of different shapes, materials and weights, it can make power grasp, precision grasp, pinch and other anthropathic actions easily. The finger control is simple and it is stable when grasping.

C. In-hand manipulation

In this subsection, an in-hand object rotation experiment is completed. With index finger and thumb working together, a sphere is rotation 30° in hand. Tennis ball diameter is 68mm and the weight is about 58g,the tennis ball can be rotate 30though work in coordination of thumb and index finger. And the sphere also can be restored to original position stably.

Though figure 16, the experiment is shown. In the process of experiments, index finger' PIP changes from 0° to 80° ,

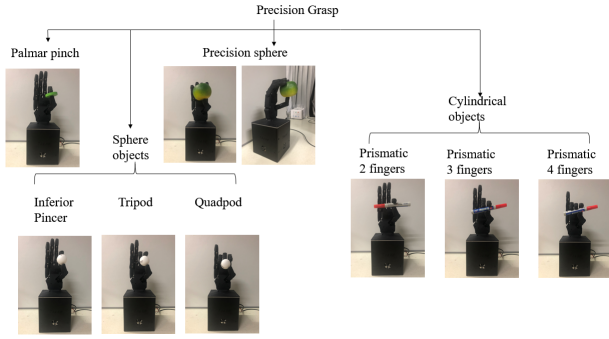


Fig. 15. The experiments of precision manipulate

DIP changes from 0° to 75° and MCP changes from 0° to 70° . In The experimental process, the ball moves smoothly.

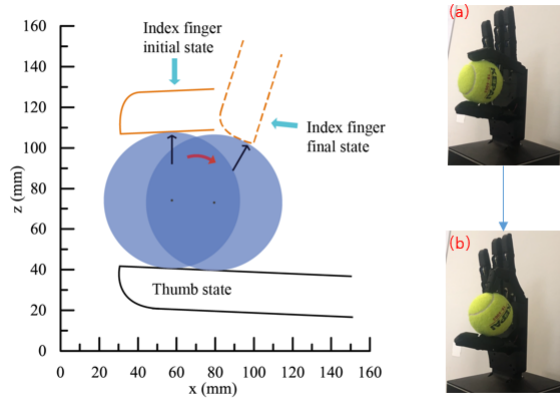


Fig. 16. Figure (a) is the initial state of index finger, (b) is the final state of index finger

D. Results

Through grasping experiments, the dexterous hand's excellent grasping ability is proved. The dexterous can achieve 19 kinds of human grasp types, include 10 kinds of power manipulations and 9 kinds of precision manipulations, enabled by the five dexterous fingers. And it can also do in-hand manipulation, this is the biggest difference between a dexterous hand and a gripper.

VI. CONCLUSIONS

This paper presents the design scheme of a 12 DoFs tendon driven dexterous hand in terms of structure and sensory system. Meanwhile a novel tension device for dexterous hand is detailed as well. This tension device not only overcomes the coupling motion between two continuous joints, but also increased motion accuracy of each finger. The performance of dexterous hand were demonstrated by a series grasping and manipulating experiments.

For the future work, based on the finger design we plan to increase DoFs of finger PIP which for abducted motion and adducted motion. Then the hand will be able to manipulate a wide variety of objects and achieve more precision in-hand manipulation. Furthermore, we will integrate more new sensors into dexterous hands to enhance the perception of dexterous hand.

ACKNOWLEDGMENT

This work is supported by National Key Research Program of China with Project No. 2018YFB1305603 and Tsinghua University Initiative Scientific Research Program No. 2019Z08QCX15.

REFERENCES

- [1] Liu, H., et al. "The modular multisensory DLR-HIT-Hand." *Mechanism and Machine Theory* 42.5(2007):612-625.
- [2] M. G. Catalano, G. Grioli, E. Farnioli, A. Serio, C. Piazza, and A. Bicchi, Adaptive synergies for the design and control of the Pisa/IIT soft-hand, *The International Journal of Robotics Research* (IJRR), vol. 33, no. 5, pp. 768C782, 2014.
- [3] Z. Ren, C. Zhou, S. Xin, and N. Tsagarakis, "HERI Hand: A Quasi Dexterous and Powerful Hand with Asymmetrical Finger Dimensions and Under Actuation," in *IEEE/RSJ International Conference on Intelligent Robots and Systems (IROS)*, 2017.
- [4] C. Marco, F. Clemente, D. Barone, A. Ghionzoli, and C. Cipriani. "The SSSA-MyHand: a dexterous lightweight myoelectric hand prosthesis." *IEEE Transactions on Neural Systems and Rehabilitation Engineering* 25, no. 5 (2017): 459-468.
- [5] A. S. Sadun, J. Jalani, F. Jamil, Grasping analysis for a 3-Finger Adaptive Robot Gripper. *IEEE International Symposium on Robotics, Manufacturing Automation*. IEEE. 2017.
- [6] L., Tommaso, J. Lipsey, and J. W. Sensinger. "The RIC Arm: A Small Anthropomorphic Transhumeral Prosthesis." *IEEE/ASME Transactions on Mechatronics (T-MECH)* 21.6 (2016): 2660-2671.
- [7] K. Xu, H. Liu, Y. Du, and Xiangyang Zhu. "Design of an underactuated anthropomorphic hand with mechanically implemented postural synergies." *Advanced Robotics* 28, no. 21 (2014): 1459-1474.
- [8] Wenliang Zhang, Bin Fang, Fuchun Sun, Mechanical design and analysis of a novel dexterous hand based on grasping manipulation, *International Conference on Robotics and Biomimetics*, 2017, 1973-1978.
- [9] C. Maxime, A. Dietrich, and M. Grebenstein. "The Thumb of the Anthropomorphic Awiwi Hand: From Concept to Evaluation." *International Journal of Humanoid Robotics* 11.03(2014):1450019.
- [10] A. Kochan, "Shadow delivers first hand", *Industrial robot: an international journal*, vol. 32, no. 1, pp. 15-16, 2005.
- [11] H. Mnyusiwalla, P. Vulliez, J.-P. Gazeau, and S. Zeghloul, "A New Dexterous Hand Based on Bio-Inspired Finger Design for Inside-Hand Manipulation," *IEEE Transactions on System, Man, and Cybernetics: Systems*, Vol. 46, NO.6, June 2016
- [12] D. H. Lee, et al. "KITECH-Hand: A Highly Dexterous and Modularized Robotic Hand." *IEEE/ASME Transactions on Mechatronics* 22.2(2017):876-887.
- [13] X. S. Jia, E. H. Adelson. "Lump Detection with a GelSight Sensor." *2013 World Haptics Conference (WHC)*. Daejeon, South Korea, IEEE, 2013: 175-179.
- [14] S. Dong, W. Yuan, et al. "Improved gelsight tactile sensor for measuring geometry and slip." *2017 IEEE/RSJ International Conference on Intelligent Robots and Systems (IROS)*. Vancouver, BC, Canada, IEEE, 2017: 137-144.
- [15] W. Yuan, A. Mandayam, et al. "Estimating object hardness with a gelsight touch sensor." *2016 IEEE/RSJ International Conference on Intelligent Robots and Systems (IROS)*. Daejeon, South Korea, IEEE, 2016: 208-215.